Ultra-strong polarization dependence of surface lattice resonances with out-of-plane plasmon oscillations

MIKKO J. HUTTUNEN,[1,*] **KSENIA DOLGALEVA,**[1,2] **PÄIVI TÖRMÄ,**[3] **AND ROBERT W. BOYD**[1,2,4]

[1]*Department of Physics, University of Ottawa, Ottawa, Ontario K1N 6N5, Canada*
[2]*School of Electrical Engineering and Computer Science, University of Ottawa, Ottawa, Ontario K1N 6N5, Canada*
[3]*COMP Centre of Excellence, Department of Applied Physics, Aalto University, P.O. Box 15100, FI-00076 Aalto, Finland*
[4]*The Institute of Optics and Department of Physics and Astronomy, University of Rochester, Rochester, New York 14627, USA*
[*]*mikkojhuttunen@gmail.com*

Abstract: The interplay between localized surface plasmon (LSP) resonances and their collective responses, known as surface lattice resonances (SLRs), in metal nanoparticle arrays can lead to resonances with high Q-factors (∼100). These responses have in the past usually been studied for LSP resonances in the plane of the array of the nanoparticles (assumed to be nonmagnetic), thus restricting efficient coupling to particles separated along a specific direction. In the present study, we demonstrate that LSPs oscillating perpendicular to the plane of the surface can lead to stronger inter-particle coupling, which enhances the SLRs. This stronger coupling occurs because the out-of-plane oscillations can couple in all directions within the plane of the array. We study the resulting SLRs for square and hexagonal lattices using the discrete-dipole approximation, and we predict much larger Q-factors in the wavelength range near 650 nm. This prediction suggests that SLRs could be very useful in enhancing various optical processes, and in many applications such as sensing and nonlinear optical wave mixing.

References and links

1. S. A. Maier, *Plasmonics: Fundamentals and Applications* (Springer, 2007).
2. L. Novotny and N. van Hulst, "Antennas for light," Nature Photon. **5**, 83–90 (2011).
3. S. Eustis and M. A. El-Sayed, "Why gold nanoparticles are more precious than pretty gold: noble metal surface plasmon resonance and its enhancement of the radiative and nonradiative properties of nanocrystals of different shapes," Chem. Soc. Rev. **35**, 209–217 (2006).
4. P. Mühlschlegel H.-J. Eisler, O. J. F. Martin, B. Hecht, and D. W. Pohl, "Resonant optical antennas," Science **308**, 1607–1609 (2005).
5. M. Pelton, J. Aizpurua, and G. Bryant, "Metal-nanoparticle plasmonics," Laser Photon. Rev. **2**, 136–159 (2008).
6. G. Vecchi, V. Giannini and J. Gómez Rivas, "Surface modes in plasmonic crystals induced by diffractive coupling of nanoantennas," Phys. Rev. B **80**, 201401 (2009).
7. K. T. Carron, W. Fluhr, M. Meier, A. Wokaun, and H. W. Lehmann, "Resonances of two-dimensional particle gratings in surface-enhanced Raman scattering," J. Opt. Soc. Am. B **3**, 430–440 (1986).
8. V. A. Markel, "Coupled-dipole approach to scattering of light from a one-dimensional periodic dipole structure," J. Mod. Opt. **40**(11), 2281–2291 (1993).
9. S. Zou, N. Janel, and G. C. Schatz, "Silver nanoparticle array structures that produce remarkably narrow plasmon lineshapes," J. Chem. Phys. **120**, 10871–10875 (2004).
10. S. Zou and G. C. Schatz, "Narrow plasmonic/photonic extinction and scattering line shapes for one and two dimensional silver nanoparticle arrays," J. Chem. Phys. **121**, 12606–12612 (2004).
11. E. M. Hicks, S. Zou, G. C. Schatz, K. G. Spears, R. P. Van Duyne, L. Gunnarsson, T. Rindzevicius, B. Kasemo, and M. Käll, "Controlling plasmon line shapes through diffractive coupling in linear arrays of cylindrical nanoparticles fabricated by electron beam lithography," Nano Lett. **5**, 1065–1070 (2005).

12. Y. Chu, E. Schonbrun, T. Yang, and K. B. Crozier, "Experimental observation of narrow surface plasmon resonances in gold nanoparticle arrays," Appl. Phys. Lett. **93**, 181108 (2008).

13. B. Auguié and W. L. Barnes, "Collective resonances in gold nanoparticle arrays," Phys. Rev. Lett. **101**, 143902 (2008).

14. V. G. Kravets, F. Schedin and A. N. Grigorenko, "Extremely narrow plasmon resonances based on diffraction coupling of localized plasmons in arrays of metallic nanoparticles," Phys. Rev. Lett. **101**, 087403 (2008).

15. L. Shi, T. K. Hakala, H. T. Rekola. J.-P. Martikainen, R. J. Moerland and P. Törmä, "Spatial coherence properties of organic molecules coupled to plasmonic surface lattice resonances in the weak and strong coupling regimes," Phys. Rev. Lett. **112**, 153002 (2014).

16. A. I. Väkeväinen, R. J. Moerland, H. T. Rekola, A.-P. Eskelinen J.-P. Martikainen, D.-H. Kim, and P. Törmä, "Plasmonic surface lattice resonances at the strong coupling regime," Nano Lett. **14**(4), 1721–1727 (2013).

17. M. Kataja, T. K. Hakala, A. Julku, M. J. Huttunen, S. van Dijken and P. Törmä, "Surface lattice resonances and magneto-optical response in magnetic nanoparticle arrays," Nat. Commun. **6**, 7072 (2015).

18. G. Vecchi, V. Giannini, and J. Gómez Rivas, "Shaping the fluorescent emission by lattice resonances in plasmonic crystals of nanoantennas," Phys. Rev. Lett. **102**, 146807 (2009).

19. P. Offermans, M. C. Schaafsma, S. R. K. Rodriguez, Y. Zhang, M. Crego-Calama, S. H. Brongersma and J. Gómez Rivas, "Universal scaling of the figure of merit of plasmonic sensors," ACS Nano **5**, 5151–5157 (2011).

20. E. M. Purcell and C. R. Pennypacker, "Scattering and absorption of light by nonspherical dielectric grains," Astrophys. J. **186**, 705–714 (1973).

21. B. T. Draine, "The discrete-dipole approximation and its application to interstellar graphite grains," Astrophys. J. **333**, 848–872 (1988).

22. J. J. Goodman, P. J. Flatau and B. T. Draine, "Application of fast-Fourier-transform techniques to the discrete-dipole approximation," Opt. Lett. **16**, 1198–1200 (1991).

23. D. Han, Y. Lai, J. Zi, Z.-Q. Zhang, and C. T. Chan, "Dirac spectra and edge states in honeycomb plasmonic lattices," Phys. Rev. Lett. **102**, 123904 (2009).

24. G. Weick, C. Woollacott, W. L. Barnes, O. Hess and E. Mariani, "Dirac-like plasmons in honeycomb lattices of metallic nanoparticles," Phys. Rev. Lett. **110**, 106801 (2013).

25. C. L. Haynes, A. D. McFarland, L. Zhao, R. P. Van Duyne, G. C. Schatz, L. Gunnarsson, J. Prikulis, B. Kasemo, and M. Käll, "Nanoparticle optics: the importance of radiative dipole coupling in two-dimensional nanoparticle arrays," J. Phys. Chem. B **107**, 7337–7342 (2003).

26. W. M. Saj, "FDTD simulations of 2D plasmon waveguide on silver nanorods in hexagonal lattice," Opt. Express **13**, 4818–4827 (2005).

27. R. Kullock, W. R. Hendren, A. Hille, S. Grafström, P. R. Evans, R. J. Pollard, R. Atkinson, and L. M. Eng, "Polarization conversion through collective surface plasmons in metallic nanorod arrays," Opt. Express **16**, 21672–21681 (2011).

28. J. Hu, C. Wang, S. Yang, F. Zhou, Z. Li, and C. Kan, "Surface plasmon resonance in periodic hexagonal lattice arrays of silver nanodisks," Nanotechnology **2013**, 838191 (2013).

29. A. D. Humphrey and W. L. Barnes, "Plasmonic surface lattice resonances on arrays of different lattice symmetry," Phys. Rev. B **90**, 075404 (2014).

30. Y.-R. Zhen, K. H. Fung, and C. T. Chan, "Collective plasmonic modes in two-dimensional periodic arrays of metal nanoparticles," Phys. Rev. B **78**, 035419 (2008).

31. W. Zhou and T. W. Odom, "Tunable subradiant lattice plasmons by out-of-plane dipolar interactions," Nat. Nanotechnol. **6**, 423–427 (2011).

32. S.-Q. Li, W. Zhou, D. B. Buchholz, J. B. Ketterson, L. E. Ocola, K. Sakoda, and R. P. H. Chang, "Ultra-sharp plasmonic resonances from monopole optical nanoantenna phased arrays," Appl. Phys. Lett. **104**, 231101 (2014).

33. H. A. Lorentz, *The Theory of Electrons and Its Applications to the Phenomena of Light and Radiant Heat*, 2nd ed. (Teubner, 1916).

34. B. T. Draine and P. J. Flatau, "Discrete-dipole approximation for scattering calculations," J. Opt. Soc. Am. A **11**, 1491-1499 (1994).

35. V. Berger, O. Gauthier-Lafaye E. Costard, "Photonic band gaps and holography," J. Appl. Phys. **82**, 60–64 (1997).

36. M. J. Huttunen, K. Lindfors, D. Andriano, J. Mäkitalo, G. Bautista, M. Lippitz, and M. Kauranen, "Three-dimensional winged nanocone optical antennas," Opt. Lett. **39**, 3686–3689 (2014).

37. Y. Yang, I. I. Kravchenko, D. P. Briggs, and J. Valentine, "All-dielectric metasurface analogue of electromagnetically induced transparency," Nat. Commun. **5**, 5753 (2014).

38. P. Törmä and W. L. Barnes, "Strong coupling between surface plasmon polaritons and emitters: a review," Rep. Prog. Phys. **78**, 013901 (2015).

39. K. Dolgaleva and R. W. Boyd, "Local-field effects in nanostructured photonic materials," Adv. Opt. Photon. **4**, 1–77 (2012).

1. Introduction

Conduction electrons near metal surfaces can couple with an incident electromagnetic field to form surface plasmons [1]. Surface plasmons excited in metal nanoparticles exhibit resonant behavior and become localized surface plasmons (LSPs), which can exhibit some interesting properties. First, the local electromagnetic field near the nanoparticles can be significantly enhanced leading to stronger light-matter interactions [1]. Second, the field can be localized down to the sub-wavelength scale, which makes it possible to control light-matter interactions at distances shorter than the traditional diffraction limit [2]. Third, the occurrence of LSPs and their resonances are influenced by the nanoparticle size, shape and environment, thus providing opportunities for various applications ranging from near-field microscopy to sensing [3–5]. However, the practical use of LSPs is often hampered by the fact that metals are intrinsically lossy at optical and near-IR wavelengths. This is especially true near the LSP resonances. The attenuation of incident radiation with wavelengths close to that of the LSP resonance could result in a significant decrease of Q-factor down to the values below 10 [6].

The Q-factors of plasmon resonances can be greatly increased by arranging the nanoparticles in periodic arrays, where the LSPs can couple with one another and exhibit collective behavior known as surface lattice resonances (SLRs) [7–14]. The collective behavior becomes stronger when the distance between the neighboring particles is an integer multiple of the incident wavelength. Such coupling between the nanoparticles in the array is often termed diffractive. An enhancement of Q-factor enabled by SLRs makes arrays of nanoparticles useful for many fundamental studies ranging from strong coupling [15,16], enhancement of weak magneto-optical Kerr effects of magnetic nanoparticles [17], to directional emission [18], or for applications such as sensing [19].

The occurrence of SLRs can be understood and accurately modelled using the discrete-dipole approximation (DDA) [7–11,16,20–22]. The inter-particle coupling is dictated by the geometrical arrangement of the nanoparticles, and numerous studies have been conducted for various array configurations such as rectangular [9, 12, 13], honeycomb [23, 24] and triangular lattices [25–29]. Yet, very little work has been done to study the effects and differences between the LSPs oscillating in the plane of the array of the nanoparticles (in-plane oscillations of LSPs) and those oscillating perpendicular to the plane of the array (out-of-plane oscillations of LSPs) and the resulting SLRs [27, 30–32].

In this Paper, we study the properties of the in-plane and out-of-plane oscillations of LSPs and the resulting SLRs in various array configurations. More specifically, we use the DDA approach to study the benefits of utilizing the out-of-plane LSPs for achieving stronger SLRs. We show that it is possible to achieve a much stronger inter-particle coupling by implementing the out-of-plane rather than in-plane oscillations of LSPs. We also propose some array geometries for SLRs that exhibit Q-factors with the values much higher than 100. We also show that the local field present in the arrays near the SLRs differs significantly from intuitive expectations based on the usual Lorentz local field [33]. We believe that our studies represent important results that could be useful for many applications, ranging from sensing to nonlinear optics.

2. Theory

2.1. *Inter-particle coupling in arrays with in-plane and out-of-plane LSP oscillations*

We first introduce the concept of a dominant nearest neighbor; this concept elucidates the difference between in-plane and out-of-plane oscillations of SLRs. We then study how the number of these dominant nearest neighbors affects the inter-particle coupling strength in 2D arrays. In traditional arrays with in-plane LSP oscillations, the current distributions associated with LSPs oscillate in the plane of the array. Therefore, LSPs of nanoparticles can efficiently couple only along one cartesian direction. Consequently, there are only two dominant nearest

neighbors that contribute to the formation of SLRs, as shown schematically for a square lattice in Fig. 1(a). This conclusion also applies to other arrangements of nanoparticles, such as hexagonal lattices [see Fig. 1(b)]. Note that this conclusion holds only for the case of non-magnetic metals such as silver and gold. In the case of magnetic nanoparticles, a dipole moment perpendicular to the plane of the nanoparticle array can be induced, and the radiation can occur in two orthogonal directions [17]. The effect is, however, weak and detectable only in the magneto-optical rather than optical response.
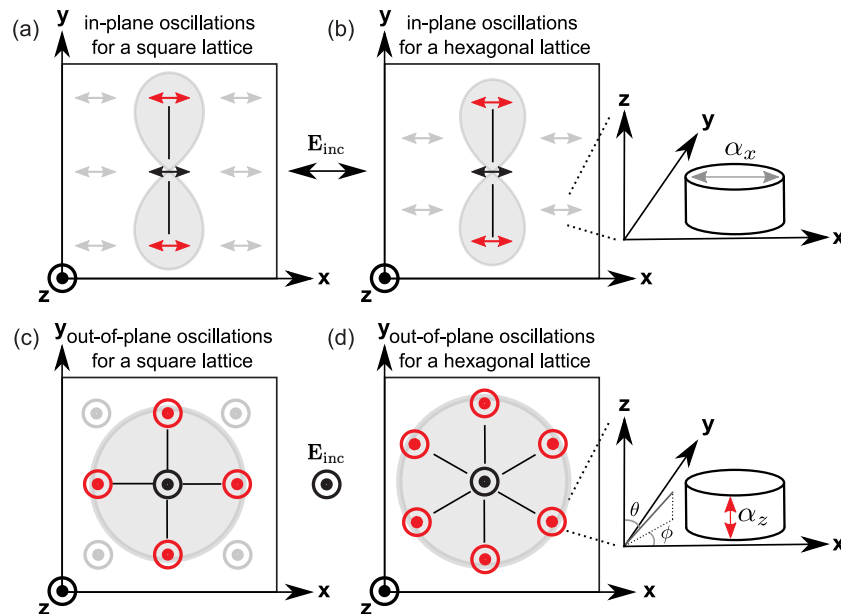

Fig. 1. Schematic diagram showing the dominant nearest neighbors for in-plane [(a) and (b)] and out-of-plane [(c) and (d)] dipole oscillations in square [(a) and (c)] and hexagonal [(b) and (d)] lattices. The light grey shaded region in each panel shows the scattering pattern of the nanoparticle at the center of the array [shown as a black arrow in (a) and (b) and a black circled dot in (c) and (d)]. Red arrows [(a) and (b)] and red circled dots [(c) and (d)] indicate the most strongly coupled nearest neighbors, and solid lines show the directions in which inter-particle coupling is strongest. Grey arrows [(a) and (b)] and grey circled dots [(c) and (d)] show neighbors for which the coupling is weak. For in-plane oscillations [(a) and (b)], strong coupling occurs only in one specific direction (indicated by solid lines), whereas for out-of-plane oscillations [(c) and (d)], strong coupling occurs in all directions within the plane of the array (as shown by solid lines). The insets schematically show the relevant polarizability components for in-plane (α_x) and out-of-plane (α_z) oscillations.

When out-of-plane oscillations of LSPs are excited, the light gets scattered equally in all directions in the plane of the array. Any given nanoparticle can thus couple efficiently with four dominant nearest neighbors in a square array, and with six dominant nearest neighbors in a hexagonal array, as shown schematically in Figs. 1(c) and 1(d), respectively. The grey shaded areas illustrate the scattering patterns of the nanoparticles at the center of the array (shown with black arrows). One can thus expect stronger diffractive coupling between the LSPs and the SLRs when out-of-plane oscillations of LSPs are excited. We discuss the benefits of the stronger coupling later in the manuscript.

2.2. Discrete-dipole approximation

A numerical approach based on the DDA has been recognized as a powerful tool for understanding the formation of SLRs [8, 9]. We chose to use this approach to study the behaviors of both in-plane and out-of-plane oscillations of SLRs for square and hexagonal array configurations. Let us consider an array of nanoparticles illuminated by an incident electromagnetic field. The field induces a dipole moment in each nanoparticle of the array. Since the dipole moment of a nanoparticle is also affected by the scattered field of other nanoparticles of the array, it is convenient to use a numerical approach to find the self-consistent dipole moments of the nanoparticles. These dipole moments can then be used to calculate the associated local field acting on the nanoparticles in the array and the extinction cross-section. The associated local field, relevant to this problem, will be later called the mesoscopic local field.

Let us assume that the incident field $\mathbf{E}_{\text{inc},j}$ at the location $\mathbf{r}_j$ of the jth scattering nanoparticle (or dipole) is a monochromatic plane wave of the form

$$\mathbf{E}_{\text{inc},j} = \mathbf{E}_0 \exp(\mathrm{i}\mathbf{k} \cdot \mathbf{r}_j - \mathrm{i}\omega t) , \tag{1}$$

where $\mathbf{E}_0$ is the electric field amplitude, $\mathbf{k} = (k_x, k_y, k_z) = (k \sin\theta \cos\phi, k \sin\theta \cos\phi, k \cos\theta)$ is the wave vector, θ is the polar angle, ϕ is the azimuthal angle [see Fig. 1(d)], and ω is the angular frequency. The incident field interacts with all the dipoles present in the array and gives rise to the total field at dipole j given by

$$\mathbf{E}_j = \mathbf{E}_{\text{inc},j} - \sum_{k \neq j} \mathbf{A}_{jk}\mathbf{p}_k , \tag{2}$$

where $\mathbf{A}_{jk}$ is a 3×3 matrix describing the interaction between the jth and k^{th} dipoles, and $\mathbf{p}_k$ is the dipole moment of the kth dipole. When the dipoles are embedded in a homogeneous medium, their dipole-dipole interaction is governed by a tensorial Green's function and can be described as [34]

$$\mathbf{A}_{jk} = \frac{\exp(\mathrm{i}kr_{jk})}{r_{jk}} \left[k^2(\hat{\mathbf{r}}_{jk}\hat{\mathbf{r}}_{jk} - \mathbf{I}_3) - \frac{1 - \mathrm{i}kr_{jk}}{r_{jk}^2}(3\hat{\mathbf{r}}_{jk}\hat{\mathbf{r}}_{jk} - \mathbf{I}_3) \right] , \quad j \neq k , \tag{3}$$

where r_{jk} is the distance between the points with coordinates $\mathbf{r}_j$ and $\mathbf{r}_k$, and $\hat{\mathbf{r}}_{jk}$ is the unit vector pointing in the direction from $\mathbf{r}_j$ to $\mathbf{r}_k$. The terms $\mathbf{I}_3$ are 3×3 identity matrices. One can also define 3×3 diagonal block matrices for the interaction matrix as $\mathbf{A}_{jj} = \alpha_j^{-1}$, where α_j is the polarizability of the jth dipole. Substituting Eq. (3) into (2), we obtain

$$\mathbf{E}_{\text{inc},j} = \mathbf{A}_{jj}\mathbf{p}_j + \sum_{k \neq j} \mathbf{A}_{jk}\mathbf{p}_k , \tag{4}$$

which can be written as a fully defined system of $3N$ linear equations with $3N$ unknown dipole moment components as

$$\mathbf{E}_{\text{inc},j} = \sum_{k=1}^{N} \mathbf{A}_{jk}\mathbf{p}_k , \tag{5}$$

provided that α_j is known. In our case, we are dealing with small identical nanoparticles, and therefore we can approximate the lineshape of each polarizability as a Lorentzian of the form [9]

$$\alpha = \frac{A_0}{(\omega_{\text{res}} - \omega) + \mathrm{i}\gamma} , \tag{6}$$

where A_0 is a constant, $\omega_{\text{res}} = 2\pi c/\lambda_{\text{res}}$ is the center frequency of the LSP resonance, c is the speed of light, and γ is the half-width of the LSP resonance. After $\mathbf{p}_j$ has been determined from

Eq. (5), the mesoscopic local field can be calculated using $\mathbf{E}_j = \alpha_j^{-1}\mathbf{p}_j$. Similarly, the extinction cross-section σ_{ext} can then be determined from

$$\sigma_{\text{ext}} = \frac{4\pi k}{|\mathbf{E}_0|^2} \sum_{j=1}^{N} \text{Im}(\mathbf{E}^*_{\text{inc},j} \cdot \mathbf{p}_j) . \tag{7}$$

2.3. Lattice sum approach

The numerical approach based on the DDA that we described in the previous section can be used to calculate the extinction cross-section and mesoscopic local field in nanoparticle arrays. These calculations can, however, become computationally intensive. An additional complication arises in the case of larger arrays ($N > 10^4$) as the computations in this case in practice require the utilization of the block Toeplitz-structure of the interaction matrix $\mathbf{A}_{jk}$ [22]. It is possible to simplify the computations for infinite arrays if the dipole moments of all the nanoparticles in the array could be considered equal to each other: ($\mathbf{p}_j = \mathbf{p}$, for all j) [9]. Then one can simplify Eq. (4) as

$$E_{\text{inc},i} = (1/\alpha_i - S)p_i , \tag{8}$$

where i refers to the Cartesian components (x, y, z) and S is the lattice sum term associated with the array. The explicit form of the lattice sum term S depends on the type of SLR and will be given later. One can then define an effective polarizability component for each nanoparticle of the array as $\alpha_i^* = p_i/E_{\text{inc},i}$ and can calculate it using Eq. (8):

$$\alpha_i^* = \frac{1}{1/\alpha_i - S} . \tag{9}$$

For in-plane oscillations of SLRs this simplification can be justified by assuming an excitation by a plane wave at normal incidence ($\theta = 0°$), because in this case the incident field is uniform in the plane of the array. The lattice sum term for arrays with in-plane oscillations $S = S_{\text{in}}$ then takes the form

$$S_{\text{in}} = \sum_{j=1}^{N} \frac{\exp(ikr_j)}{r_j} \left[k^2 \sin^2 \vartheta_j + \frac{(1 - ikr_j)(3 \cos^2 \vartheta_j - 1)}{r_j^2} \right] , \tag{10}$$

where the sum extends over N nearest neighboring dipoles, r_j is the distance to the jth dipole, and ϑ_j is the angle between $\mathbf{r}_j$ and the dipole moment component p_i.

In order to excite out-of-plane oscillations of SLRs, an optical field at an oblique angle of incidence θ is required to couple light into the out-of-plane LSPs. In this case, both in-plane and out-of-plane oscillations of SLRs get excited, as the incident field has both in-plane and out-of-plane components. Then the incident field at the sites of the array dipoles is no longer uniform due to the non-zero in-plane wave vector components k_x and k_y. The condition for the simplification of the computations, requiring the equality of all the dipole moments in the array, thus cannot be exactly fulfilled. In our calculations, we use for simplicity an incoming wave with the angle of incidence $\theta = 0.0001°$. Then $\mathbf{E}_{\text{inc},j} \approx \mathbf{E}_0$, and we assume that the coupling to the in-plane LSPs is weak and can be neglected. We discuss the validity of this assumption in the Discussions section of the manuscript. With these assumptions, and by noting that $\vartheta_j = 90°$ for all j, one can simplify the lattice sum term for arrays with out-of-plane oscillations $S = S_{\text{out}}$ to the form

$$S_{\text{out}} = \sum_{j=1}^{N} \frac{\exp(ikr_j)}{r_j} \left[k^2 - \frac{1 - ikr_j}{r_j^2} \right] . \tag{11}$$

Once the effective polarizability α^* has been determined, the extinction cross-section can be calculated using [21]

$$\sigma'_{\text{ext}} = 4\pi k N \sum_i \text{Im}(\alpha_i^*) \,, \tag{12}$$

where we use the prime symbol to emphasize the difference between this result and Eq. (7). Here, we assume that the polarizabilities of all dipoles are equal, whereas in the DDA approach the effective polarizabilities are allowed to vary.

3. Results and discussion

In order to demonstrate the appearance of SLRs and to study their dispersion, we calculated the extinction cross-section as a function of the incident photon energy and the inverse array period $q = 2\pi/a$ for the square and hexagonal lattices with in-plane and out-of-plane oscillations of LSPs. We varied the array period a from 300 to 700 nm and calculated the extinction cross-section using the lattice sum approach and Eq. (12). These calculations were performed under the assumption that each scattering nanoparticle with a LSP resonance at 515 nm is equally excited by the incident field. The parameters $A_0 = 0.4 \text{ cm}^3/\text{s}$ and $\gamma = 3.18 \times 10^{14} \text{ s}^{-1}$ were chosen by finding a close agreement between the simulated and previously measured [16] extinction spectra from silver nanoparticle arrays. The surrounding medium was assumed homogeneous with a refractive index of $n = 1.51$, and the number of scattering nanoparticles was set at $N = 210 \times 210$. The results are shown in Fig. 2, where we plot the extinction cross section as a function of the incident photon energy. One can see the larger avoided crossings between the modes for the out-of-plane oscillations. This observation suggests that out-of-plane oscillating LSPs are coupled more strongly. The largest avoided crossing occurs for out-of-plane oscillations in a hexagonal array, and this observation agrees well with the intuitive explanation of the coupling provided in Fig. 1.

In order to better explain these results, we plot in Fig. 3(a) the extinction spectra for square and hexagonal arrays with the lattice constants $a_{\text{in, squ}} = 430$ nm, $a_{\text{out, squ}} = 435$ nm, $a_{\text{in, hex}} = 500$ nm and $a_{\text{out, hex}} = 505$ nm. The subscripts "in" and "out" refer to in-plane and out-of-plane oscillations of LSPs, while "squ" and "hex" signify square and hexagonal arrays. The lattice constants were selected in such a way that a narrow SLR near 1.9 eV (~650 nm) appears. The slightly different lattice constants were chosen to slightly separate the peaks in the figure to make it easier to deduce which resonances are stronger. The results corresponding to these lattice constants are also marked in Fig. 2 with dark grey, red, blue and light grey dashed lines, respectively. In order to compare the lattice sum results with those obtained using the more rigorous approach, we also calculated the corresponding extinction spectra using the DDA method, as described in Section 2.2 [see Fig. 3(b)]. We recall that in order to excite the out-of-plane oscillations of LSPs, one has to set the angle of incidence of the incoming optical field slightly off normal with respect to the surface of the array. In our DDA calculations, we chose the angle of incidence of the incoming optical field to make 0.0001° with the normal to the surface of the array, and set the polarization of the incident field to be in the plane of the incidence. In order to compare the relative strengths of the resulting SLRs, the calculated extinction cross-sections for in- and out-of-plane resonances were normalized with respect to the excitation field component E_x and E_z, respectively. These results can be understood in terms of the lattice sums S and S_{out}, which are plotted together with $1/\alpha$ in Fig. 3(c). Strong SLRs occur when the real parts of the lattice sums and $1/\alpha$ cross, maximizing the extinction cross-section [see Eqs. (9) and (12)].

The results shown in Figs. 2 and 3 confirm our expectations that out-of-plane LSPs could lead to stronger SLRs. For an equal number of scattering particles N, the maximum value for the lattice sum S_i was achieved when the out-of-plane resonances were excited, as seen in Fig. 3(c). Therefore, the out-of-plane resonances exhibit stronger inter-particle coupling resulting
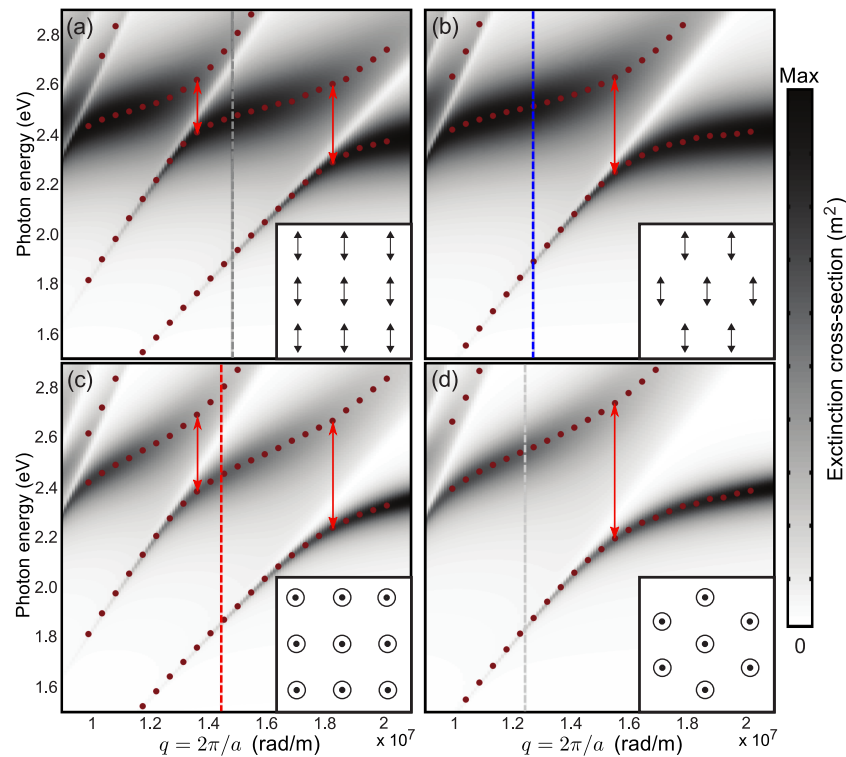
Fig. 2. Extinction cross-section as a function of the incident photon energy and the inverse array periodicity $q = 2\pi/a$, plotted for (a) in-plane square, (b) in-plane hexagonal, (c) out-of-plane square, and (d) out-of-plane hexagonal arrays. Dark-red filled circles follow the local maxima of the extinction and display the dispersion relation of the resonances. For the out-of-plane resonances, the stronger inter-particle coupling results in larger avoided crossings between the modes, visualized by red arrows. The special cases treated in Fig. 3 are indicated by colored dashed lines.

in stronger SLRs, as one can see from Figs. 3(a) and 3(b). This stronger coupling is also seen as the larger avoided crossings between the modes (see red arrows in Fig. 2).

We also studied how the mesoscopic local field experienced by individual nanoparticles of the array, is affected by the SLRs. The maximum local-field-enhancement factors for the previously described square and hexagonal arrays are shown in Fig. 3(d). The results are normalized with respect to the incident field amplitudes. As one can see from the graph, the mesoscopic local field is enhanced much more strongly near the SLRs with peaks around 1.9 eV, rather than in the vicinity of the LSP resonances (~2.5 eV). The out-of-plane SLRs for the square and hexagonal arrays give the strongest local-field-enhancement factors of 3.7 and 2.9, respectively. Since it is the mesoscopic local field that is responsible for light-matter interactions, identifying the mechanisms of local-field enhancement should be useful for various applications such as nonlinear optics where the outcome of the light-matter interaction scales as several powers of the local-field enhancement factor.

Next, we discuss how the incident light could be coupled more efficiently to the out-of-plane SLRs. We recall that our results were normalized to the strongest field component of the incident field responsible for coupling light into the SLR of interest. In the case of the out-of-plane SLRs, the amplitude of this field component is small, and therefore stronger coupling schemes are desired to fully exploit the out-of-plane resonances. Let us first consider square arrays of
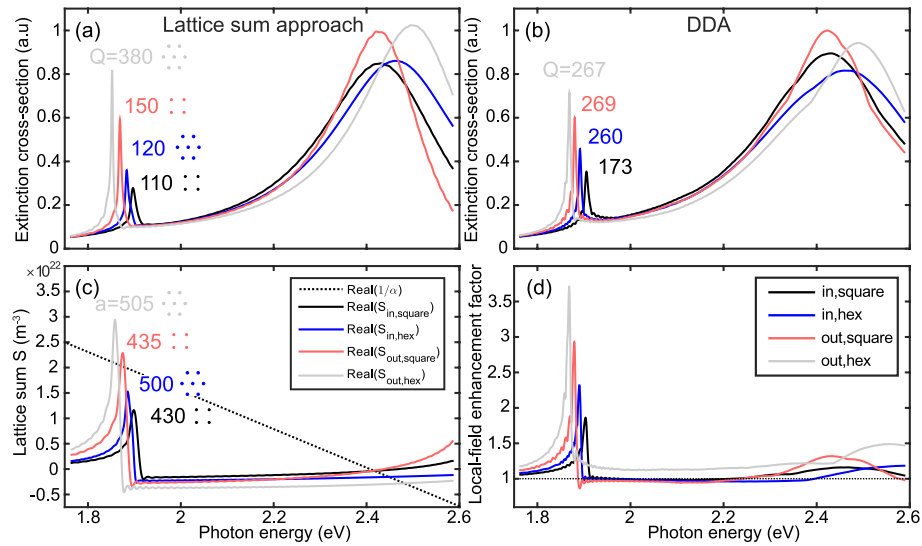
Fig. 3. The extinction spectra for the array periods of a = 430 nm, 500 nm, 435 nm, and 505 nm, calculated using the lattice sum approach (a) and DDA (b). The slightly different periods were chosen to separate the peaks on the graph for better clarity. The calculated Q-factors of the SLRs are shown next to their corresponding peaks in (a) and (b). These results can be understood in terms of the lattice sums, shown in (c). Strong SLRs occur when the real part of the lattice sum S_i and $1/\alpha$ (shown with the dotted line) cross. Therefore, larger lattice sums can give rise to stronger SLRs. The enhancement of the mesoscopic local field acting on an individual nanoparticle by the array and its resonances is shown in (d).

nanoparticles. In this case, the simplest solution that leads to increased coupling efficiency is simply to change the angle of incidence slightly from the surface normal of the array ($\theta \neq 0°$). Then, by properly choosing the value of θ, one could make the phase accumulation of the field between the adjacent nanoparticles [due to the term exp($i\mathbf{k} \cdot \mathbf{r}$)] equal to a multiple of 2π near the SLR wavelength, and SLRs can be excited. But this phase accumulation is detrimental to the Q-factors of the SLRs. An improvement can be made through adding another plane wave incident at an angle $-\theta$ in the plane of incidence of the first wave. The superimposed fields form a standing wave in the plane of the array. The cumulative effect of the amplitude and the phase variation restores the possibility for achieving SLRs with high Q-factor values. In addition, if the second wave is out-of-phase with respect to the first one, the in-plane field components of the superimposed fields cancel out, making the coupling into the out-of-plane oscillations dominant [see Fig. 4(a)]. A similar approach can also work for hexagonal arrays, where the total of three tilted incident plane waves with the azimuthal angles ϕ varying in the multiples of 120° should be used [see Fig. 4(b)]. We note that similar excitation schemes have been used before, for example, in photolithography, and should be fairly straightforward to implement [35].

Another way of increasing the coupling efficiency is to design the nanoparticles in such a way that the incoming optical field at normal incidence couples more efficiently to LSPs associated with the out-of-plane current oscillations. One such potential nanoparticle design could be, for example, three-dimensional winged nanocones, which have previously been shown to efficiently couple transverse far-field radiation to strong out-of-plane oscillations in the structures [36].

Finally, we discuss the implications and potential applications of our results. It is clear from Figs. 3(a) and 3(b) that out-of-plane SLRs can lead to moderate and high-Q resonances, which could be beneficial for improving the figures of merit in sensing [19]. But one should recall that our results predict the behavior of larger arrays with $N = 210 \times 210$ particles corresponding to
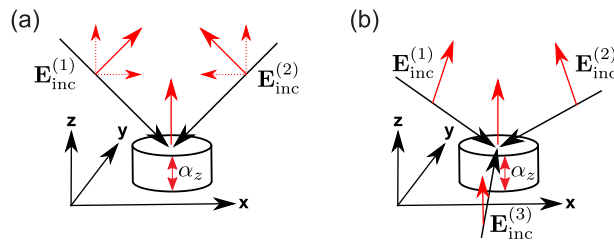
Fig. 4. More efficient coupling schemes for (a) square and (b) hexagonal arrays with out-of-plane oscillations. (a) If the incident fields are out-of-phase, the in-plane (out-of-plane) field component of the incident waves interfere destructively (constructively), thus making the coupling into out-of-plane oscillations dominant. (b) Similar to square lattices, hexagonal lattices can be efficiently excited using three incident fields.

physical array size of $\sim 100 \times 100$ μm^2. This physical size might limit the applicability of the arrays for sensing in case much smaller sensing areas are required. Reducing the array size, on the other hand, will decrease the Q-factor values of the SLRs [37]. Therefore, there is a trade-off between the highest achievable Q-factor and the sensor size. Our results could also be useful in strong coupling studies, since out-of-plane SLRs show larger avoided crossings than the more traditional in-plane SLRs [16]. In addition, the strong mesoscopic local field [see Fig. 3(d)] is also expected to enhance the coupling between the SLRs and emitters placed in the vicinity of the nanoparticles [38].

Another particularly interesting application of stronger SLRs is for nonlinear optics. Since nonlinear optical interactions scale as several powers of the excitation field, the local-field enhancements due to the geometric lattice effects could significantly enhance the generated nonlinear optical signals. For example, our perhaps moderate-seeming maximum local-field enhancement of 3.7 is already considerably larger than the usual Lorentz local field correction estimated for homogeneous materials [39] and corresponds to a $\sim$190-fold ($\sim$25 000-fold) increase in the intensity of the nonlinear processes scaling with the square (third power) of the fundamental field oscillating at frequency ω. However, care should be taken when our results, which apply to what is effectively a two-dimensional system, are compared with the usual Lorentz local field corrections based on homogeneous three-dimensional systems. Moreover, since these results were achieved without a full optimization of the parameters for the local-field enhancement, further increase can be expected with a more careful design of the arrays. We also note that the calculated local-field enhancement arises from the geometrical effect due to the array, and we did not take into account an additional near-field enhancements near the nanoparticles due to the presence of LSP resonances. This could also be considered in future studies.

4. Conclusions

In conclusion, we have systematically studied the collective responses of plasmonic metal nanoparticle arrays known as surface lattice resonances. We used two computational approaches: a more rigorous approach, based on discrete-dipole approximation, and a simple analytical dipole-sum approach, to study the differences in the inter-particle coupling for the cases where the surface plasmons of the particles oscillate either in the plane of the array or perpendicular to it. Our studies have shown that the coupling between the nanoparticles is, in general, stronger for out-of-plane oscillations. We have performed our studies for both square and hexagonal lattices, and have shown that the coupling is stronger for the hexagonal arrays, in agreement with our intuitive explanation of the underlying physics. The resulting surface lattice resonances have been shown to have high Q-factor values in the visible wavelength range. In addition, it has been shown

that the collective array response could strongly modify the local field acting on the individual elements of the array. This mesoscopic local field has also been shown to be considerably different from the usual predictions based on Lorentz local field and assuming homogeneous media. We believe that our results could be useful for various applications, including sensing, strong coupling studies, and nonlinear optics.